

# The 2.5 Å X-ray crystal structure of the acid-stable proteinase inhibitor from human mucous secretions analysed in its complex with bovine $\alpha$ -chymotrypsin

Markus G.Grütter<sup>1</sup>, Gabriele Fendrich<sup>1</sup>, Robert Huber and Wolfram Bode

Max-Planck-Institut für Biochemie, D-8033 Martinsried, FRG and <sup>1</sup>Ciba-Geigy AG, Pharmaceutical Division, CH-4002 Basel, Switzerland

Communicated by R.Huber

**Orthorhombic crystals of the complex formed between bovine  $\alpha$ -chymotrypsin and a recombinant human mucous proteinase inhibitor (SLPI) were grown. Data to 2.3 Å resolution were collected on the area-detector diffractometer FAST. The crystal structure of the complex was solved by Patterson search techniques using chymotrypsin as a search model. A cyclic procedure of modeling and crystallographic refinement enabled the determination of the SLPI structure. The current crystallographic R-value is 0.19. SLPI has a boomerang-like shape with both wings comprising two well separated domains of similar architecture. In each domain the polypeptide chain is arranged like a stretched spiral. Two internal strands form a regular  $\beta$ -hairpin loop which is accompanied by two external strands linked by the proteinase binding segment. The polypeptide segment of each domain is interconnected by four disulfide bridges with a connectivity pattern hitherto unobserved. The reactive site loop of the second domain has elastase and chymotrypsin binding properties. It contains the scissile peptide bond between Leu72I and Met73I and has a similar conformation to that observed in other serine proteinase protein inhibitors. Eight residues of this loop, two of the adjacent hairpin loop, the C-terminal segment and Trp-30I are in direct contact with the cognate enzyme. The binding loop of the first domain (probably with anti-trypsin activity) is disordered due to proteolytic cleavage occurring in the course of crystallization.**

**Key words:** antileukoprotease/crystal structure/chymotrypsin complex/human proteinase inhibitor

## Introduction

Several acid-stable low mol. wt proteinase inhibitors, with high affinity for trypsin and chymotrypsin as well as for leukocyte elastase and cathepsin G, have been found in human mucous fluids, such as seminal plasma (Haendle *et al.*, 1965; Fink *et al.*, 1971; Schiessler *et al.*, 1976), cervical mucus (Wallner and Fritz, 1974), bronchial (Hochstrasser *et al.*, 1972; Ohlsson *et al.*, 1977) and nasal secretions (Hochstrasser *et al.*, 1971), tears (Küppers, 1971) and salivary glands (Ohlsson *et al.*, 1983). According to inhibitory characteristics, molecular mass, immunological cross reactivity, amino acid composition (Schiessler *et al.*, 1978; Klasen and Kramps, 1985; Smith and Johnson, 1985) and (if available) amino acid sequences, the major inhibitory

species of these mucous fluids seem to be derived from a single polypeptide (Seemüller *et al.*, 1986; Thompson and Ohlsson, 1986) of mol. wt 12 kd.

Due to subsequent proteolytic cleavages occurring *in vivo* and *in vitro*, various multiple forms have been found in the different fluids after purification. Depending on the tissue of origin these inhibitors have been called human seminal plasma inhibitor I (HUSI-I), cervix uteri secretion inhibitor (CUSI), bronchial secretory inhibitor (BSI), bronchial mucus inhibitor (BMI), bronchial leukocyte proteinase inhibitor (BLPI) or secretory leukocyte protease inhibitor (SLPI). The common origin from mucous fluids of all these related inhibitor species suggests the term mucous proteinase inhibitor (MPI). However, the term SLPI will be used in this paper.

Its physiological function seems to be protection of the mucosal epidermis against degradation by liberated proteolytic enzymes, especially those contained in granulocytic lysosomes. Due to its inhibitory activity against serine proteinases, this inhibitor was also called antileukoprotease (ALP). It deserves interest as a possible therapeutic agent to be used in local inflammatory processes.

The complete amino acid sequence of HUSI-I/SLPI was recently established by two groups working independently: (i) by a combination of peptide and DNA sequencing techniques applied to proteolytically modified forms of HUSI-I and to a cloned cDNA derived from human cervical tissue (Seemüller *et al.*, 1986; Heinzel *et al.*, 1986, 1987), and (ii) by peptide sequencing of an intact inhibitor chain from human parotid secretions (Thompson and Ohlsson, 1986; Ohlsson *et al.*, 1987) and subsequent cDNA sequencing (Stetler *et al.*, 1986). Accordingly, this inhibitor consists of a single polypeptide chain of 107 amino acid residues and 11 726 daltons mol. wt. Significant sequence homologies were found only with whey proteins from rat (Dandekar *et al.*, 1982) and mouse (Hennighausen and Sippell, 1982) and with the second domain of the basic inhibitor from Red Sea Turtle (Kato and Tominaga, 1979). It has been shown that the N-terminal and the C-terminal halves of the peptide chain display internal sequence homology, obeyed exactly by the eight cysteine residues of each domain involved in disulfide bond formation. From the preferred cleavage sites, domain organization and inhibition spectrum two reactive sites were proposed.

In order to evaluate the SLPI polypeptide fold, its spatial organization in two domains and its disulfide connectivity, and to determine unequivocally its reactive sites and their interaction with target enzymes, we have tried to crystallize SLPI complexes with serine proteinases. We have obtained well-diffracting single crystals of the 1:1 complex formed with bovine  $\alpha$ -chymotrypsin and have subsequently determined its structure applying X-ray crystallographic techniques. In this paper we present the unique peptide fold of the SLPI chain, its organization within two separate domains, its hitherto unobserved disulfide pattern, the reactive site conformation of the second domain and its interaction with the

bound enzyme. The detailed structure and experimental details will be described elsewhere.

## Results

Figure 1 shows the  $\alpha$ -carbon drawing of the MPI–chymotrypsin complex. The inhibitor component binds with its second domain (see below) into the substrate-binding region of the enzyme. The main chain of the  $\alpha$ -chymotrypsin component can be traced from Cys1 to Gly12 (activation peptide), from Ile16 to Tyr146 and from Ala149 to the C-terminal Asn245. The r.m.s. deviation of all  $\alpha$ -carbon atoms from those of free  $\gamma$ -chymotrypsin (Cohen *et al.*, 1981) and of the  $\alpha$ -chymotrypsin-dimer (Tsukuda and Blow, 1985) is  $\sim 0.4$  Å.

The SLPI main chain (inhibitor residues are designated by an I after the sequence number) shows no ordered electron density at both the amino (Ser1I) and the carboxy termini (Lys106I, Ala107I). In addition peptide segment Ser15I to Lys23I cannot be traced in the Fourier maps, and the adjacent residues Lys13I, Lys14I and Pro24I are only poorly defined. This disorder is probably the result of proteolytic cleavage near the reactive site of the first SLPI domain. Its conformation is therefore inferred from the second domain. Except for these regions the electron density map is in agreement with the published SLPI amino acid sequence and, in addition, establishes the so far unknown disulfide connectivities.

The N- and the C-terminal halves of the SLPI chain are organized in two distinct domains (Figures 1 and 2). The MPI molecule exhibits the shape of a boomerang, with both knobs representing the enzyme binding regions. After optimal superposition of both domains the residues of peptide fragment 5I–51I are topologically equivalent to 59I–105I. The r.m.s. deviation of all  $\alpha$ -carbon atoms of both fragments (excluding segments 13I–24I and 67I–78I) is 0.7 Å. Domain 1 can be transformed onto domain 2 by a screw operation with a rotation of about  $150^\circ$  and a translation of about 16 Å along the rotation axis. The domain boundary is at Asp52I, with residues 1I to Val51I forming the first and Thr53I to Ala107I the second domain.

Besides the covalent connection there are only a few

additional noncovalent contacts between both domains, most of them contributed by the N-terminal (Lys3I to Gly8I) and the C-terminal (Ser100I to Val102I) segments which cross and form the main chain hydrogen bonds between Phe5I and Cys101I. Phe79I, Gln85I and Lys87I of the second domain interact with Trp30I and Arg37I of the first domain (Figure 1). The disulfides form intra-domain bridges only.

As shown in Figure 3 for the second domain only, each domain exhibits the shape of a flat wedge, with the pointed edge formed by the enzyme-binding loop. The polypeptide chain is arranged like a stretched planar spiral which contains four anti-parallel extended segments connected by three curved polypeptide loops. The two exterior straight chain segments (A and B, Figure 2), which are part of the N-terminal half of each domain are in the second domain connected by the wide loop between Tyr68I and Leu74I which contains the primary enzyme-binding segment and the reactive site bond. Beneath this wide loop is a narrow hairpin loop linking both interior strands (C and D, Figure 2) made up of the C-terminal half of each domain. Strand B is further connected through a helical segment with the internal strand C, while the other internal (D) and external (A) strands are linked through loop segments with the second or first domain respectively (Figures 1 and 2). These latter loops opposite to the enzyme-binding loop are partly stacked upon one another making this domain end globular.

The connectivity of the four straight strands (Figure 2) can be topologically designated as +3, –2, +1 (Richardson, 1981). However, they do not form a regular hydrogen-bonded  $\beta$ -pleated sheet; only both internal strands form a double-stranded twisted  $\beta$ -sheet connected by five main-chain hydrogen bonds. The two strands are joined by a two-residue (Sibanda and Thornton, 1985) or four-residue class 2 (Milner-White and Poet, 1986)  $\beta$ -hairpin loop (Figures 2 and 3). No hydrogen bond is formed between the parallel strands A and C and only one between strands B and D (Figure 2).

Strands A and C are involved in several contacts through side chains which act more like spacers than connectors. Most of their peptide groups are oriented perpendicular to the 'sheet' plane and make polar interactions with fixed solvent molecules. The loop between B and C is coiled and

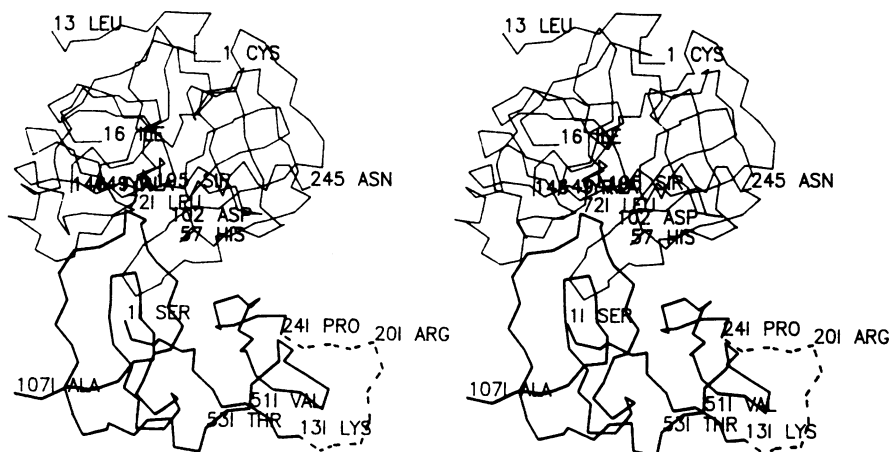


**Fig. 1.**  $\alpha$ -Carbon drawing of the complex formed by bovine  $\alpha$ -chymotrypsin (thin connections) and human MPI (bold connections). The MPI segment Lys13I to Pro24I of the first SLPI domain which is poorly defined in the electron density map is given in dashed lines. Only residues terminating covalent peptide segments, the active site residues of  $\alpha$ -chymotrypsin and the PI residue of the second SLPI domain are labeled.

contains two to three consecutive tight turns (Figures 2 and 4).

Each of the internal strands is covalently connected through disulfide bridges with one (D–B) or both (C–A and C–B) outer strands. A fourth disulfide bridge links the proteinase-binding loop with the adjacent hairpin loop. Three of the four disulfides (26I–38I, 10I–39I, 32I–37I in the first and 80I–92I, 64I–93I, 86I–101I in the second domain) are spatially close and knot all four peptide strands together by a covalent network in the centre of each domain.

The small number of hydrophobic amino acid residues in the domain core is remarkable (Figures 2 and 4); aromatic side chains are completely absent with the exception of Phe79I which is involved in inter-domain contacts. In contrast, the core comprises several polar residues some of which are buried and involved in intra-domain hydrogen bonds and electrostatic interactions (see Figure 4). The side chains of Lys60I and Lys6I for example are virtually buried and their ammonium groups placed in the centre of three to four main chain carbonyl groups donated by the coiled segments Asp83I to Leu90I and Asp29I to Lys36I respectively; also, the side chains of Asp29I and Asp83I are internal and engaged in salt linkages with Arg37I and the homologous Lys91I respectively. SLPI exhibits with 12 prolines per 107 residues an exceptionally high proline content. All of these

proline residues are in *trans*-conformation; at two proline pairs (Pro11I–Pro12I and Pro76I–Pro77I) the peptide chain adopts a polyproline II-like conformation (Figure 4).

Most of the inhibitor contacts with the cognate enzyme are made by eight residues Thr67I to Leu74I, the 'primary' binding segment (Figures 4 and 5). Few additional intermolecular contacts are contributed by Met96I and Cys97I, i.e. two residues of the 'secondary' binding segment connected by disulfide 71I–97I to the primary loop. Besides this binding region of the second domain, only the C-terminal segment (Val102I) and the indole side chain of Trp30I (i.e. a residue of the first domain!) are engaged in intermolecular van der Waals contacts with the enzyme (Figures 1 and 5). The conformation of the primary binding segment around the scissile peptide bond [especially from P2 to P1', using the substrate and binding site nomenclature suggested by Schechter and Berger (1967)] and its association with main-chain segments of chymotrypsin (Figure 5) are very similar to those previously observed for other serine proteinase complexes with protein inhibitors [as listed e.g. by Bode *et al.* (1987)]. P1-residue Leu72I is located in the primary specificity pocket (S1). As the S1 pocket is incompletely occupied by the Leu72I side chain, several solvent molecules are enclosed and can be localized. This is similar to the  $\alpha$ -chymotrypsin complex formed with the ovomucoid third

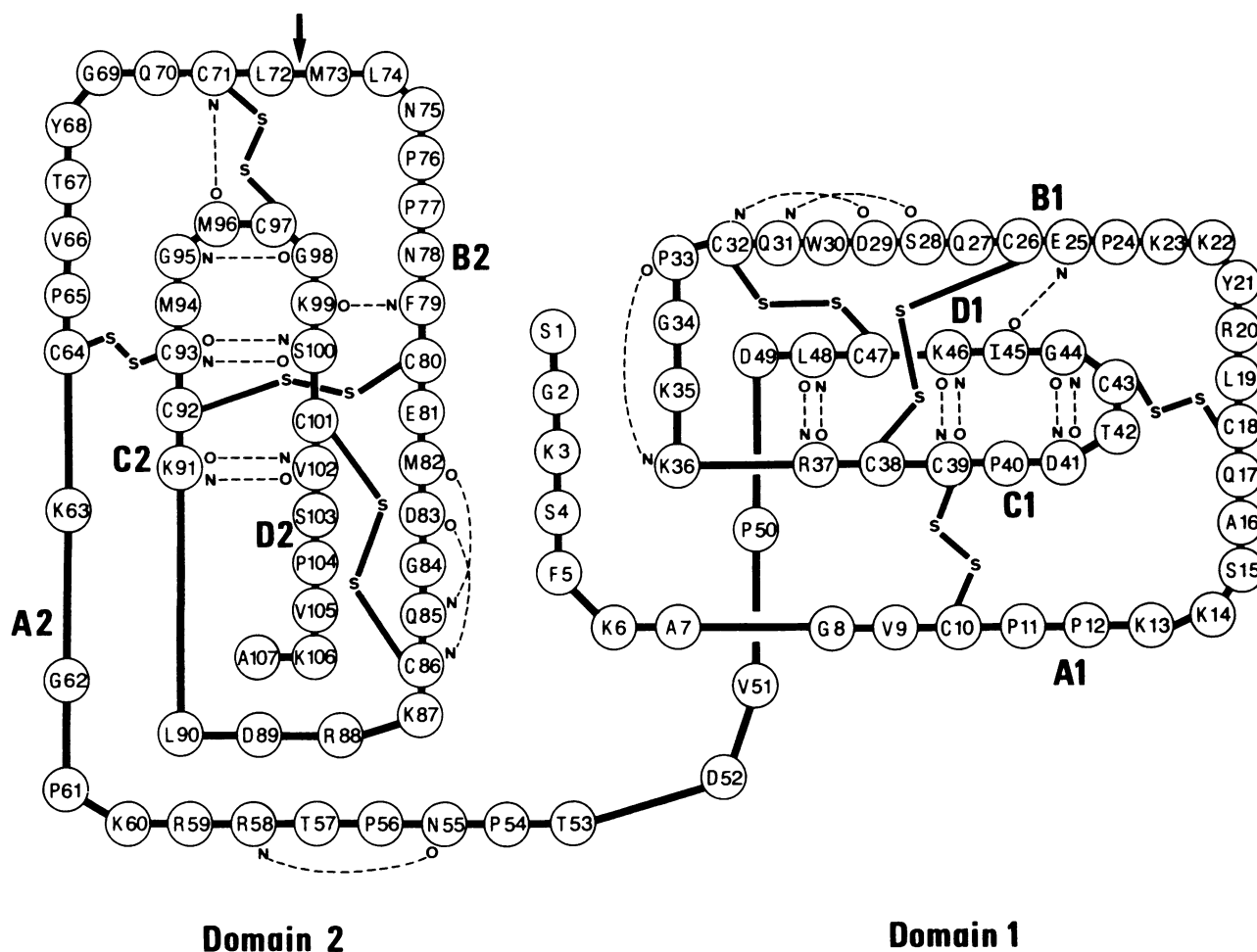


**Fig. 2.** Schematic representation of the polypeptide chain arrangement of human SLPI and its disulfide connectivities. Inter-main-chain hydrogen bonds displayed by dashed lines were selected for the current model according to definitions (using energy cut-off values of  $-0.5$  kcal/mol) given by Kabsch and Sander (1983). The arrow indicates the scissile peptide bond of domain 2.

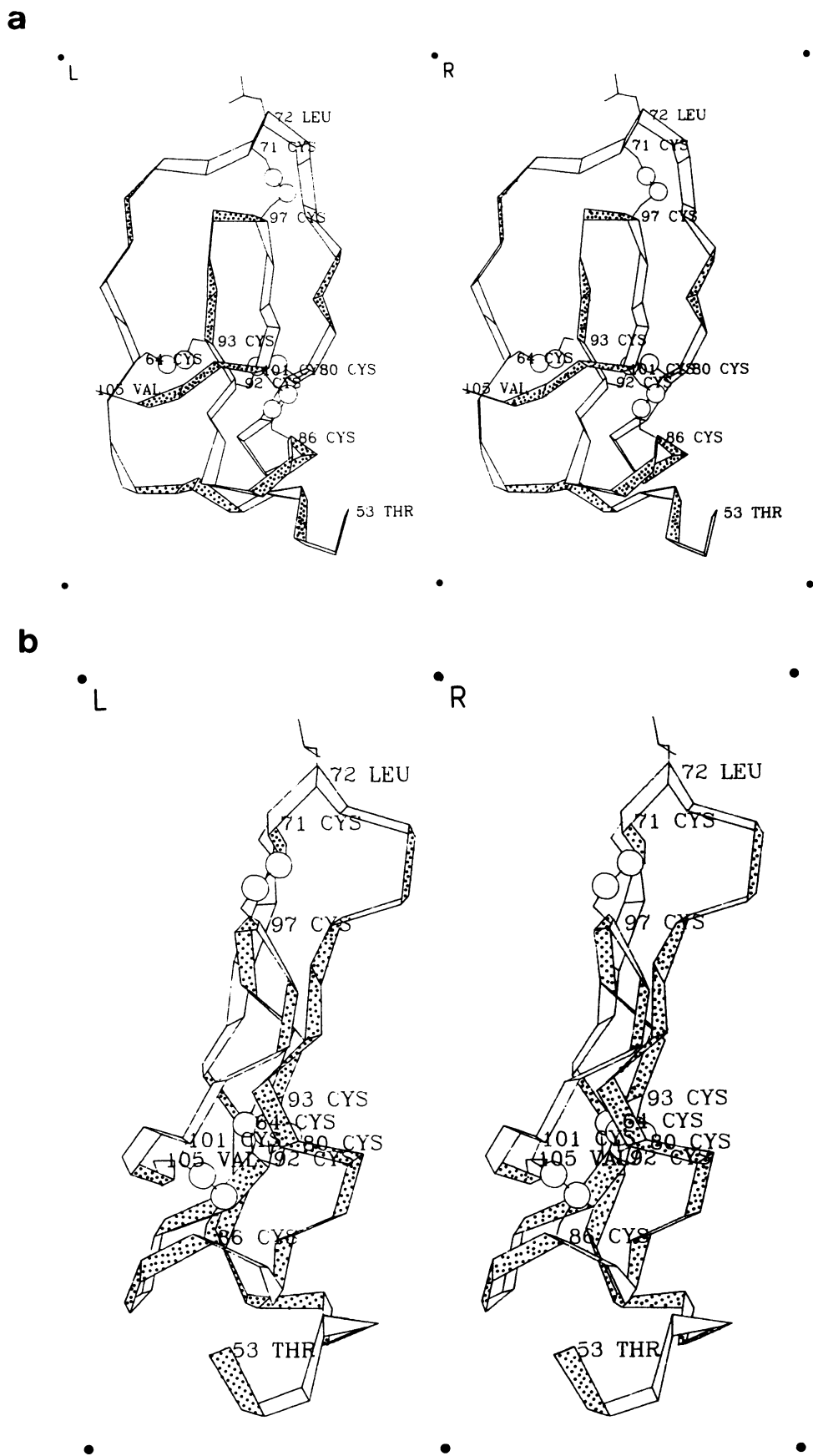


**Fig. 3.** Ribbon diagram of the polypeptide chain of the second SLPI domain, with creases at each  $\alpha$ -carbon position. Only P1 residue Leu721 and the eight cysteine residues of this domain (with the sulfur atoms represented by large spheres) are fully shown. (a) 'Front' view, similar to Figures 1 and 4. (b) 'Side' view, after a 90° rotation around a vertical axis. Figures are prepared with a program written by Lesk and Hardman (1982).

domain from turkey (Fujinaga *et al.*, 1987), which has also a Leu at P1. Two methionine residues, Met74I and Met96I, are in direct contact with residues of chymotrypsin through their side chains.

The scissile peptide bond Leu72I–Met73I is intact, and its carbonyl carbon is in van der Waals contact with Ser195 OG. The side chain of the preceding residue Gln70I points towards this peptide bond (Figures 4 and 5). The NE2 atom of its carboxamide group is engaged in two (relatively long) hydrogen bonds with the carbonyl groups of Cys71I and Met73I, which are in opposite direction to the carbonyl group of the scissile bond.

## Discussion

As already suggested on the basis of internal sequence homology (Seemüller *et al.*, 1986; Heinzl *et al.*, 1986, 1987; Thompson and Ohlsson, 1986; Ohlsson *et al.*, 1987) the SLPI polypeptide chain is organized in two domains of similar folding. The X-ray analysis now reveals its spatial organization in two well separated domains and its boomerang-like shape. In contrast, the double-headed serine proteinase inhibitor of the Bowman–Birk type (Suzuki *et al.*, 1987) exhibits a more elongated shape with both independent proteinase binding sites on opposite ends. The small number of contacts between both SLPI domains suggests that they are independent folding domains. The high degree of spatial similarity despite different interdomain contacts (heterol-

ogous association) corroborates this view. This idea will have to be verified by domain separation or domain synthesis.

The SLPI molecule represents a new and hitherto unobserved polypeptide folding motif. Each domain is composed of a spirally arranged polypeptide chain. Only the internal (C-terminal) part of the spiral is organized in a regular two-stranded  $\beta$ -sheet (37I–48I and 81I–102I) with a hairpin turn. The N-terminal part which forms the primary binding segment surrounds this  $\beta$ -sheet and is connected to it through a disulfide bridge, two hydrogen bonds and a few hydrophobic contacts generating an unusually flat structure (Figure 3b). The chain organization is the more surprising as most of the side chains of the residues forming the proteinase-binding loop of the second domain are of hydrophobic nature but project away from the molecular core. Remarkably the core is not predominantly hydrophobic but has buried charged residues as described before. In the polypeptide segments located opposite to the binding loop more common structural motifs are found, like tight turns with inter-main-chain hydrogen bonds and charge–charge interactions including side chains.

The disulfide connection pattern of SLPI was established by this X-ray structure analysis. All disulfide bridges are inter-domain links. The cysteine content (8 cysteines/58 amino acid residues) in SLPI is rather high. Other 'small disulfide-rich' proteins containing four cysteines per domain (Drenth *et al.*, 1980) are known. Among them the spatial structures of wheat germ agglutinin (Wright, 1987) and three

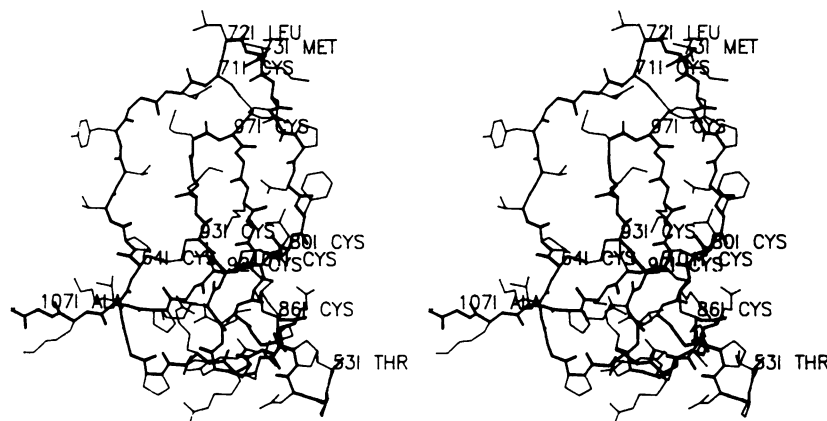


Fig. 4. Complete structure of the second SLPI domain. Main chain atom connections are emphasized by bold lines.

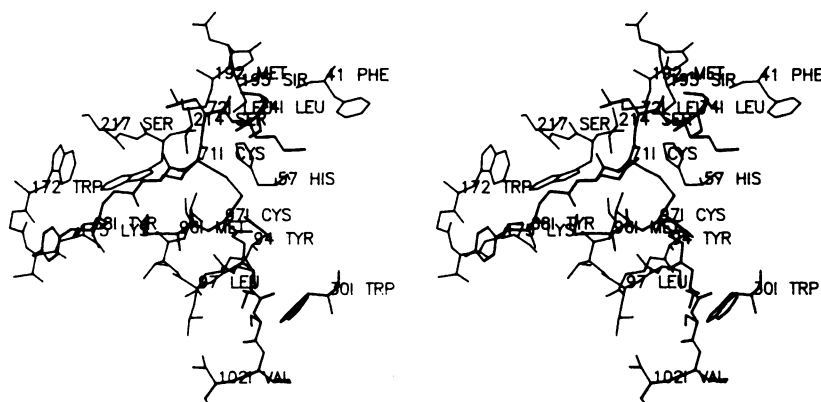


Fig. 5.  $\alpha$ -Chymotrypsin–SLPI second domain interface from a similar view as used in Figures 1, 3 and 4. Polypeptide chain segments of SLPI are given by bold lines, chymotrypsin segments by thin lines.

sea snake neurotoxins (Low *et al.*, 1976; Tsernoglou and Petsko, 1976) were elucidated. On the basis of similar cysteine distribution patterns it has been suggested that the SLPI chain might be similarly organized and disulfide cross-connected (Heinzel, 1987). As shown here this is not correct. Instead, SLPI is the member of a new family of 'four-disulfide core proteins'. The close sequence homology of SLPI with the two whey proteins (Dandekar *et al.*, 1982; Hennighausen and Sippel, 1982) and the second domain of the Red Sea Turtle inhibitor (Kato and Tominaga, 1979) suggests similar three-dimensional structures and disulfide connectivities.

The present analysis defines the exact position of the reactive site of the second SLPI domain as Leu72I–Met73I. The conformation of the proteinase-binding loop of the second SLPI domain and its interaction with surrounding active site residues of the cognate enzyme is similar to that found in other 'small' proteinase inhibitors but resembles particularly BPTI (Deisenhofer and Steigemann, 1975; Huber and Bode, 1978) which also carries a cysteine at P2 (Cys14). Preliminary model building experiments show that SLPI also fits to the binding site of human leukocyte elastase (Bode *et al.*, 1986) without requiring large conformational changes. The relative orientation of the adjacent disulfide-linked loop is, however, opposite in SLPI and BPTI. The carboxamide group of Gln70I in SLPI is involved in hydrogen bond interactions with carbonyl groups on both sides of the scissile peptide bond (i.e. of the P2 and P1' residues) and resembles Asn33 in the Kazal-type inhibitors, which, however, stems from the secondary binding loop (Weber *et al.*, 1981). The close packing of the side chains of two methionine residues (Met74I and Met96I) against the enzyme explains the oxidation sensitivity of the anti-elastase property of SLPI (Carp and Janoff, 1980).

The analogous chain segment Lys13I to Pro24I of the first domain is disordered but is likely to have a similar conformation. Disorder precludes an exact definition of the scissile bond, but from a comparison of both SLPI domains it should be either Leu19I–Arg20I or Arg20I–Tyr21I. Antitryptic behavior of this domain suggests the latter alternative. This implies a shift of one residue with respect to the adjacent cysteine, which in turn would require a different conformation of the disulfide bridge, perhaps more similar to the Kazal-type inhibitors (Weber *et al.*, 1981). Lys13I and Pro24I of the first domain are topologically similar to Thr67I and Asn78I. Under the assumption that trypsin binds to the first SLPI domain similar to chymotrypsin binding to the second SLPI domain without inducing large conformational changes, SLPI should be able to bind both enzymes simultaneously.

The structure of SLPI highlights a general problem of folding and stability of small disulfide-rich proteins. SLPI has no hydrophobic core and very little internally hydrogen bonded secondary structure. It is difficult to understand that the observed polypeptide fold is also the conformation of minimal free energy in the absence of disulfide bonds. On the other hand, the correct formation of the disulfide linkages at reasonable rates requires relative stability of the observed conformation also in the reduced state. The diversity of folding motifs observed in small disulfide-rich proteins is remarkable and emphasizes the enormous versatility of proteins.

## Materials and methods

Human recombinant SLPI was obtained from Synergen Inc., Boulder, CO. It was further purified by gel filtration on Sephadex G-50 superfine in 2% (v/v) acetic acid. According to SDS–PAGE it is at least 95% homogeneous and migrates according to an apparent mol. wt of 13 500 daltons. Bovine  $\alpha$ -chymotrypsin (EC 3.4.4.5) of CDI grade was purchased from Worthington. A stoichiometric complex between SLPI and  $\alpha$ -chymotrypsin was formed by adding both components at a 1.1:1 molar ratio. This complex was crystallized in 1.6 M phosphate, pH 6.2, at 20°C using the hanging drop vapor diffusion method. These crystals are of orthorhombic space group P2<sub>1</sub>2<sub>1</sub>2<sub>1</sub>; the cell constants are a = 66.90 Å, b = 70.24 Å, c = 86.05 Å. They contain one (complex) molecule per asymmetric unit and diffract to about 2.0 Å resolution.

X-ray intensity data were collected with a FAST television area detector diffractometer (Enraf–Nonius, Delft). Ni-filtered CuK $\alpha$  radiation was produced by a Rigaku rotating anode generator operated at 5.4 kW with an apparent focal spot of 0.3 × 0.3 mm. The diffractometer is equipped with a device that allows cooling of the crystal samples to 4°C. Two different crystals were rotated about their b\* and c\* axes for about 90°. Frames with a width of 0.1° were taken for 100 s. The crystal-to-film distance was 45 mm, allowing collection of intensity data to a maximal resolution of about 2.3 Å. The data were evaluated on-line using the program system MADNES (Messerschmidt and Pflugrath, 1987) as described by Huber *et al.* (1987). The measured intensity data were processed and merged using PROTEIN (Steigemann, 1974).

Significantly measured reflections (62 792) to 2.3 Å resolution were processed yielding 13 119 independent reflections. The reflections to 2.5 Å account for 81% of all reflections expected. The shell from 2.5 Å to 2.6 Å resolution was 50% complete. The R<sub>merge</sub> defined as  $\Sigma(I - \langle I \rangle) / \Sigma I$  is 0.091.

The orientation of the chymotrypsin component in the crystals was determined by Patterson search techniques (Huber, 1965) as implemented in PROTEIN using intensity data to 3.5 Å resolution and the refined model of  $\gamma$ -chymotrypsin (Cohen *et al.*, 1981) as deposited at the Brookhaven Data Bank (Bernstein *et al.*, 1977). The three-dimensional correlation function between the Patterson maps of the model and the observed intensity data had a highest value of 6 $\sigma$  above the mean. The second highest peak was 4.5 $\sigma$  above the mean. The highest value represented the correct orientation. The positioning of the chymotrypsin molecule in the unit cell was achieved using the translation function of Crowther and Blow (1967) and programs written by E.E.Lattmann and modified by J.Deisenhofer and R.Huber. Translation functions of the three Harker sections were calculated and showed the highest peaks at consistent locations. Rotational and translational parameters were further refined by a Fourier transform fitting program TRAREF (Huber and Schneider, 1985).

A 3 Å 2F<sub>o</sub>–F<sub>c</sub> Fourier map calculated with sigma-a weighted (Read, 1986) model phases and further improved by solvent flattening displayed the chymotrypsin molecule and in addition showed electron density representing most of the inhibitor component. The binding segment of the second SLPI domain comprising ~15 residues was modeled against the Fourier map on a PS330 interactive display system (Evans and Sutherland) using the PSFRODO version (Pflugrath *et al.*, 1984) of FRODO (Jones, 1978). The current model was partially refined using EREF (Jack and Levitt, 1978). The new sigma-a weighted Fourier map allowed modeling of additional parts of the SLPI chain which were included in subsequent refinement steps. This cyclic procedure was repeated several times under stepwise increase of the resolution to 2.5 Å. The current model includes main-chain atoms of  $\alpha$ -chymotrypsin segments Cys1 to Gly12, Ile15 to Tyr146, Ala149 to Asn245, of SLPI segments Lys3I to Pro12I, Glu25I to Val105I and about 50 stereochemically reasonable localized solvent molecules. The current R-value (defined as  $\Sigma(|F_o| - |F_c|) / \Sigma |F_o|$ ) for 11 734 data from 25 Å to 2.5 Å resolution is 0.19. The total energy of the model is –1097 kcal/mol. The r.m.s. deviations from ideal values for bond lengths and bond angles are 0.017 Å and 2.6° respectively.

## Acknowledgements

We thank Professor Hans Fritz for valuable suggestions, Professor J. Nüesch for his kind support of this project, and Drs M.Young and R.C.Thompson (Synergen, Boulder, Co) for the preparation of human recombinant SLPI. This work has been financially supported by the Sonderforschungsbereich 207 of the Deutsche Forschungsgemeinschaft.

## References

- Bernstein, F.C., Koetzle, T.F., Williams, G.J.B., Meyer, E.F., Jr, Brice, M.D., Rodgers, J.R., Kennard, O., Shimanouchi, T. and Tasumi, M. (1977) *J. Mol. Biol.*, **112**, 535–543.
- Bode, W., Papamokos, E. and Musil, D. (1987) *Eur. J. Biochem.*, **166**, 673–692.
- Bode, W., Wei, A.-Z., Huber, P., Meyer, E., Travis, J. and Neumann, S. (1986) *EMBO J.*, **5**, 2453–2458.
- Carp, H. and Janoff, A. (1980) *Exp. Lung Res.*, **1**, 225–237.
- Cohen, G.H., Silverton, E.W. and Davies, D.R. (1981) *J. Mol. Biol.*, **148**, 449–479.
- Crowther, R.A. and Blow, D.M. (1967) *Acta Crystallogr. Sect. A*, **23**, 544–548.
- Dandekar, A.M., Robinson, E.A., Appella, E. and Qasba, P.-K. (1982) *Proc. Natl. Acad. Sci. USA*, **79**, 3987–3991.
- Deisenhofer, J. and Steigemann, W. (1975) *Acta Crystallogr. Sect. B*, **31**, 238–250.
- Drenth, J., Low, B.W., Richardson, J.S. and Wright, C.S. (1980) *J. Biol. Chem.*, **255**, 2652–2655.
- Fink, E., Jaumann, E., Fritz, H., Ingrisch, H. and Werle, E. (1971) *Hoppe-Seyler's Z. Physiol. Chem.*, **352**, 1591–1594.
- Fujinaga, M., Sielecki, A.R., Read, R.J., Ardelt, W., Laskowski, M., Jr and James, M.N.G. (1987) *J. Mol. Biol.*, **195**, 397–418.
- Haendle, H., Fritz, H., Trautschold, I. and Werle, E. (1965) *Hoppe-Seyler's Z. Physiol. Chem.*, **343**, 185–187.
- Heinzel, R. (1986) Ph.D. Thesis, Technische Hochschule, Darmstadt.
- Heinzel, R., Appelhans, H., Gassen, G., Seemüller, U., Machleidt, W. and Steffens, G. (1986) *Eur. J. Biochem.*, **106**, 61–67.
- Heinzel, R., Appelhans, H., Gassen, H.-G., Seemüller, U., Arnhold, M., Fritz, H., Lottspeich, F., Wiedenmann, K. and Machleidt, W. (1987) In Taylor, J.C. and Mittman, C. (eds), *Pulmonary Emphysema and Proteolysis: 1986*. Academic Press, New York, pp. 297–306.
- Hennighausen, L.G. and Sippel, A.E. (1982) *Nucleic Acids Res.*, **10**, 2677–2684.
- Hochstrasser, K., Haendle, H., Reichert, R. and Werle, E. (1971) *Hoppe-Seyler's Z. Physiol. Chem.*, **352**, 954–958.
- Hochstrasser, K., Reichert, R., Schwarz, S. and Werle, E. (1972) *Hoppe-Seyler's Z. Physiol. Chem.*, **353**, 221–226.
- Huber, R. (1965) *Acta Crystallogr. Sect. A*, **19**, 353–356.
- Huber, R. and Bode, W. (1978) *Acc. Chem. Res.*, **11**, 114–122.
- Huber, R. and Schneider, M. (1985) *J. Appl. Crystallogr.*, **18**, 165–169.
- Huber, R., Schneider, M., Epp, O., Mayr, I., Messerschmidt, A., Pflugrath, J. and Kayser, H. (1987) *J. Mol. Biol.*, **195**, 423–434.
- Jack, A. and Levitt, M. (1978) *Acta Crystallogr. Sect. A*, **34**, 931–935.
- Jones, A. (1978) *J. Appl. Crystallogr.*, **11**, 268–272.
- Kabsch, W. and Sander, C. (1983) *Biopolymers*, **22**, 2577–2637.
- Kato, I. and Tominaga, N. (1979) *Fed. Proc.*, **38**, 832.
- Klasen, E.C. and Kramps, J.A. (1985) *Biochem. Biophys. Res. Commun.*, **128**, 285–289.
- Lesk, A.M. and Hardman, K.D. (1982) *Science*, **216**, 539–540.
- Messerschmidt, A. and Pflugrath, J. (1987) *J. Appl. Crystallogr.*, **20**, 306–315.
- Küppers, F. (1971) *Biochim. Biophys. Acta*, **229**, 845–849.
- Low, B.W., Preston, H.S., Sato, A., Rosen, L.S., Searl, J.E., Rudko, A.D. and Richardson, J.S. (1976) *Proc. Natl. Acad. Sci. USA*, **73**, 2991–2994.
- Milner-White, E.J. and Poet, R. (1986) *Biochem. J.*, **240**, 289–292.
- Ohlsson, K., Tegner, H. and Akesson, U. (1977) *Hoppe-Seyler's Z. Physiol. Chem.*, **358**, 583–589.
- Ohlsson, M., Rosengren, M., Tegner, H. and Ohlsson, K. (1983) *Hoppe-Seyler's Z. Physiol. Chem.*, **364**, 1323–1328.
- Ohlsson, K., Rosengren, M., Stetler, G., Brewer, M., Hale, K.K. and Thompson, R.C. (1987) In Taylor, J.C. and Mittman, C. (eds), *Pulmonary Emphysema and Proteolysis: 1986*. Academic Press, New York, pp. 307–324.
- Pflugrath, J.W., Saper, M.A. and Quioco, F.A. (1984) In Hall, S. and Ashiaka, T. (eds), *Methods and Application in Crystallographic Computing*. Clarendon Press, Oxford, p. 407.
- Read, R.J. (1986) *Acta Crystallogr. Sect. A*, **42**, 140–149.
- Richardson, J.S. (1981) *Adv. Prot. Chem.*, **34**, 167–340.
- Schechter, I. and Berger, A. (1967) *Biochem. Biophys. Res. Commun.*, **27**, 157–162.
- Schiessler, H., Arnhold, M., Ohlsson, K. and Fritz, H. (1976) *Hoppe-Seyler's Z. Physiol. Chem.*, **357**, 1251–1260.
- Schiessler, H., Hochstrasser, K. and Ohlsson, K. (1978) In Havemann, K. and Janoff, A. (eds), *Neutral Proteases of Human Polymorphonuclear Leucocytes*. Urban and Schwarzenberg, Baltimore, pp. 195–207.
- Seemüller, U., Arnhold, M., Fritz, H., Wiedenmann, K., Machleidt, W., Heinzel, R., Appelhans, H., Gassen, H.-G. and Lottspeich, F. (1986) *FEBS Lett.*, **199**, 43–48.
- Sibanda, B.L. and Thornton, J.M. (1985) *Nature*, **316**, 170–174.
- Smith, C.E. and Johnson, D.A. (1985) *Biochem. J.*, **225**, 463–472.
- Steigemann, W. (1974) Ph.D. Thesis, Technische Universität, München.
- Stetler, G., Brewer, M.T. and Thompson, R.C. (1986) *Nucleic Acids Res.*, **14**, 7883–7896.
- Suzuki, A., Tsunogae, Y., Tanaka, I., Yamane, T., Ashida, T., Norioka, S., Hara, S. and Ikenaka, T. (1987) *J. Biochem.*, **101**, 267–274.
- Thompson, R.C. and Ohlsson, K. (1986) *Proc. Natl. Acad. Sci. USA*, **83**, 6692–6696.
- Tsernoglou, D. and Petsko, G.A. (1976) *FEBS Lett.*, **68**, 1–4.
- Tsukuda, H. and Blow, D.M. (1985) *J. Mol. Biol.*, **184**, 703–711.
- Wallner, O. and Fritz, H. (1974) *Hoppe-Seyler's Z. Physiol. Chem.*, **355**, 709–715.
- Weber, E., Papamokos, E., Bode, W., Huber, R., Kato, I. and Laskowski, M., Jr (1981) *J. Mol. Biol.*, **149**, 109–123.
- Wright, C.S. (1987) *J. Mol. Biol.*, **194**, 501–529.

Received on November 16, 1987